

All in one: Nanoparticles are involved in many fields of research and many realisations and expectations rely on them. Indeed, nanoparticles can be used as supports regardless of the application. Thus, methods have to be set up to fulfil the goal of multi-functionality. The developments in the field of multi-functional nanoparticles (MFNPs) are presented and discussed.



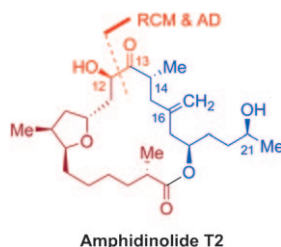
Metathesis

T. Perrier, P. Saulnier,
J.-P. Benoit* 11516–11529

Methods for the Functionalisation of Nanoparticles: New Insights and Perspectives

COMMUNICATIONS

RCM + AD = T2: In the presence of the C16-methylene group, regioselective ring-closing metathesis (RCM) formed the (12*E*)-endocyclic double bond, which underwent Os-catalyzed asymmetric dihydroxylation (AD) to give the desired 12,13-diol intermediate required for the total synthesis of amphidinolide T2 in 16 linear steps in 8.0% overall yield.



Total Synthesis

*H. Li, J. Wu, J. Luo,
W.-M. Dai** 11530–11534

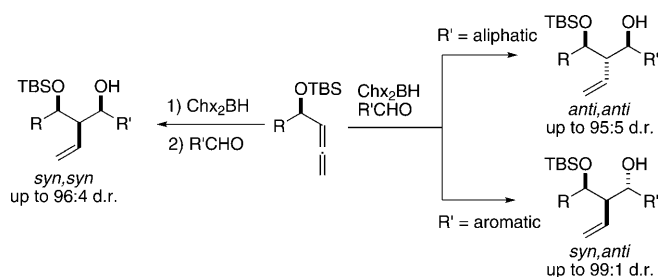
A Concise Total Synthesis of Amphidinolide T2



Asymmetric Synthesis

C. Sánchez, X. Ariza, J. Cornellà,
J. Farràs, J. Garcia,*
J. Ortiz* 11535–11538

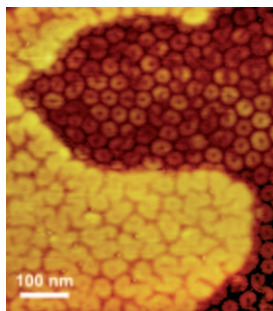
Stereodivergent Addition of 4-Silyloxy-1,2-Allenes to Aldehydes by Hydroboration



All-ene one! Three out of four stereoisomers of 2-vinyl-1,3-diols can be obtained from a single allene. A simple variation of the reaction conditions modifies the stereochemical outcome of the addition of an allene to an

aldehyde via hydroboration. Stereocontrol is dependent upon the order in which the reagents are mixed (leading to *E* or *Z* boron species) and the type of aldehyde (aliphatic or aromatic) used.

Fluorine in bloom: A nonpolar fluorocarbon/hydrocarbon tetrablock self-assembles into a first monolayer consisting of an array of densely packed discrete circular surface micelles (dark); this layer is surmounted by a second layer of such nano-objects (light).



Self-Assembly

*C. de Gracia Lux,
M. P. Krafft** 11539–11542

Nonpolar Gemini Amphiphiles Self-Assemble into Stacked Layers of Nano-Objects



Energy Storage

L. Ji, Z. Lin, B. Guo, A. J. Medford,
X. Zhang* 11543–11548

Assembly of Carbon–SnO₂ Core–Sheath Composite Nanofibers for Superior Lithium Storage



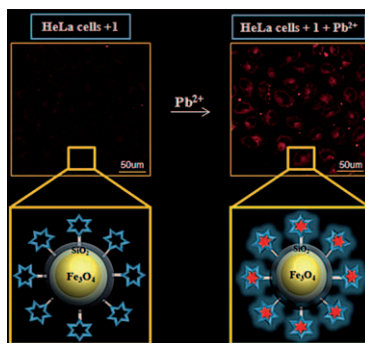
Protective coating: Carbon–SnO₂ core–sheath composite nanofibers are synthesized through the creative combination of electrospinning and electrodeposition processes (see figure).

They display excellent electrochemical performance when directly used as binder-free anodes for rechargeable lithium ion batteries.

Chemosensors

H. Son, H. Y. Lee, J. M. Lim,
D. Kang,* W. S. Han, S. S. Lee,
J. H. Jung* 11549–11553

A Highly Sensitive and Selective Turn-On Fluorogenic and Chromogenic Sensor Based on BODIPY-Functionalized Magnetic Nanoparticles for Detecting Lead in Living Cells

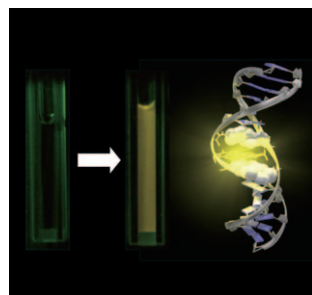


A new fluoro-chromogenic chemosensor based on BODIPY-functionalized Fe₃O₄@SiO₂ core/shell nanoparticles **1** has been prepared. Chemosensor **1** exhibits a high affinity and selectivity for Pb²⁺ over competing metal ions tested. Moreover, confocal microscopy, and flow cytometry experiments established that **1** can be used for detecting Pb²⁺ levels within living cell.

Fluorescent Probes

H. Kashida, K. Sekiguchi,
H. Asanuma* 11554–11557

Insulator Base Pairs for Lighting-up Perylene-3,4,9,10-tetracarboxylic diimide in a DNA Duplex

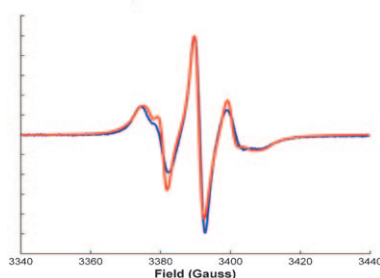
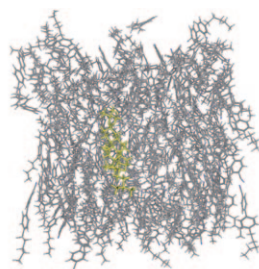


Quenched: Perylene-3,4,9,10-tetracarboxylic diimide (PDI) is highly quenched by nucleobases, which greatly restricts its application as a fluorescent probe. Here, we propose “insulator base pairs” tethering cyclohexane ring through D-threoninol. When “insulator base pairs” were inserted between PDI and nucleobases, the quantum yield of PDI drastically increased several thousand-fold. The “insulator base pairs” reported here also have the potential to increase the quantum yields of other fluorophores.

Molecular Dynamics Simulations

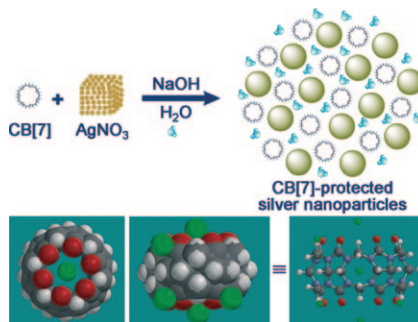
E. Kuprusevicius, R. Edge, H. Gopee,
A. N. Cammidge, E. J. L. McInnes,
M. R. Wilson,
V. S. Oganessian* 11558–11562

Prediction of EPR Spectra of Liquid Crystals with Doped Spin Probes from Fully Atomistic Molecular Dynamics Simulations: Exploring Molecular Order and Dynamics at the Phase Transition



Liquid crystals spin their secrets: Electron paramagnetic resonance (EPR) spectra are predicted directly and completely from fully atomistic molecular dynamics (MD) simulations of 4-cyano-4-*n*-pentylbiphenyl (5CB) nematic liquid crystals with a doped nitroxide spin probe (depicted in yellow; red curve = simulated and blue curve = measured EPR spectrum).

Silver nanoparticles made easy: A simple, effective, and one-pot method toward the synthesis of a defined macrocycle–silver nanoparticle system in water has been described (see figure). Interestingly, cucurbituril (CB)[7]-protected AgNPs showed significantly increased cytotoxicity against MCF-7 and NCI-H358 cancer cells, as demonstrated by models in vitro.

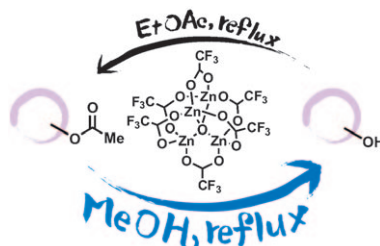


Silver Nanoparticles

*T. Premkumar, Y. Lee, K. E. Geckeler** 11563–11566

Macrocycles as a Tool: A Facile and One-Pot Synthesis of Silver Nanoparticles Using Cucurbituril Designed for Cancer Therapeutics

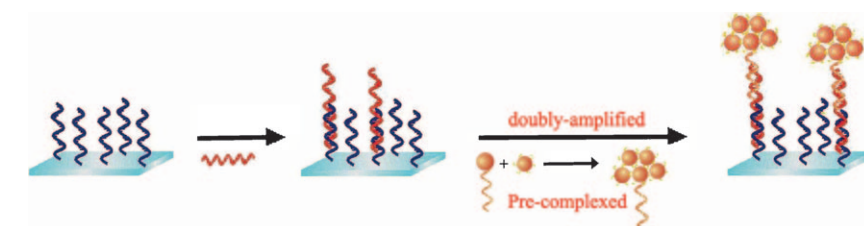
A new catalytic deacylation of acetates and benzoates through transesterification with methanol was developed (see scheme). Reactions with various acid- and nucleophile-sensitive functional groups proceeded efficiently in the presence of a catalytic amount of the tetranuclear zinc cluster. The present catalysis is applicable to less-reactive tertiary acetates, the deacylation of which is difficult to achieve by transesterification with other catalysts.



Homogeneous Catalysis

T. Iwasaki, K. Agura, Y. Maegawa, Y. Hayashi, T. Ohshima, K. Mashima** 11567–11571

A Tetranuclear-Zinc-Cluster-Catalyzed Practical and Versatile Deprotection of Acetates and Benzoates



Easy detection: The target DNA in a 10–100 am range can be detected by pre-complexed nanoparticles without additional amplification or target labeling. The $[\text{Ru}(\text{bpy})_3]^{2+}$ -doped silica nanoparticles are hybridized to form a

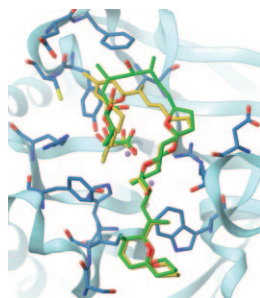
complex with highly enhanced sensitivity (see scheme). This method will be a significant improvement over conventional microarray/fluorescence readout systems.

DNA Sensors

S. W. Bae, M. S. Cho, S.-S. Hur, C.-B. Chae, D. S. Chung, W.-S. Yeo, J.-I. Hong** 11572–11575

A Doubly Signal-Amplified DNA Detection Method Based on Pre-Complexed $[\text{Ru}(\text{bpy})_3]^{2+}$ -Doped Silica Nanoparticles

Toxin precursors: Corozalic acid, a new Ser/Thr protein phosphatase 1 and 2A inhibitor that turned out to be a key metabolic intermediate, was isolated from cultures of the marine dinoflagellate *Prorocentrum belizeanum*. Detailed spectroscopic analysis and extensive computational calculations revealed its structure and conformational behavior. In addition, a comprehensive picture of the interactions of corozalic acid with PP1 and PP2A is proposed (see figure) on the basis of ab initio, docking and molecular dynamics calculations.



Natural Products

J. G. Napolitano, M. Norte, J. J. Fernández,* A. Hernández Daranas** 11576–11579

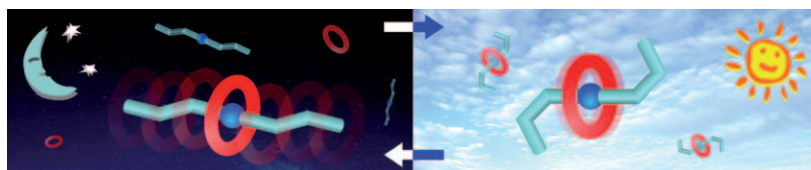
Corozalic Acid: A Key Okadaic Acid Biosynthetic Precursor with Phosphatase Inhibition Activity

FULL PAPERS

Photochemistry

M. Baroncini, S. Silvi, M. Venturi,
A. Credi* 11580–11587

Reversible Photoswitching of Rotaxane Character and Interplay of Thermodynamic Stability and Kinetic Lability in a Self-Assembling Ring–Axle Molecular System



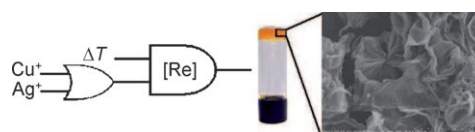
By night one way, by day another: Clear-cut, facile, and reversible switching between the thermodynamically stable pseudorotaxane form and the kinetically inert rotaxane form (see

figure) is obtained by light irradiation of a self-assembling system composed of a macrocycle and a thread molecule equipped with azobenzene end groups.

Organogels

S.-T. Lam,
V. W.-W. Yam* 11588–11593

Synthesis, Characterisation and Photo-physical Study of Alkynylrhenium(I) Tricarbonyl Diimine Complexes and Their Metal-Ion Coordination-Assisted Metallogelation Properties



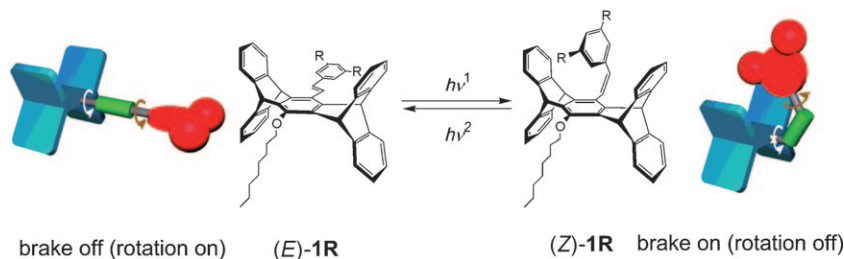
Gelled together: A series of alkynyl-rhenium(I) tricarbonyl diimine complexes has been synthesised and shown

to display rich thermotropic gelation behaviour upon Cu^I or Ag^I coordination (see scheme).

Molecular Devices

W.-T. Sun, Y.-T. Huang, G.-J. Huang,
H.-F. Lu, I. Chao,* S.-L. Huang,
S.-J. Huang, Y.-C. Lin, J.-H. Ho,
J.-S. Yang* 11594–11604

Penttiptycene-Derived Light-Driven Molecular Brakes: Substituent Effects of the Brake Component



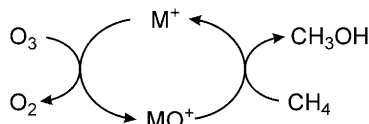
Putting on the brakes: Stilbene-based molecular brakes reduce the rotation rate of the penttiptycene rotor by 10⁶–10⁹-fold, depending on the brake size,

on going from the brake-off ((*E*)-**1**) to the brake-on ((*Z*)-**1**) states through reversible photoisomerization reactions (see graphic).

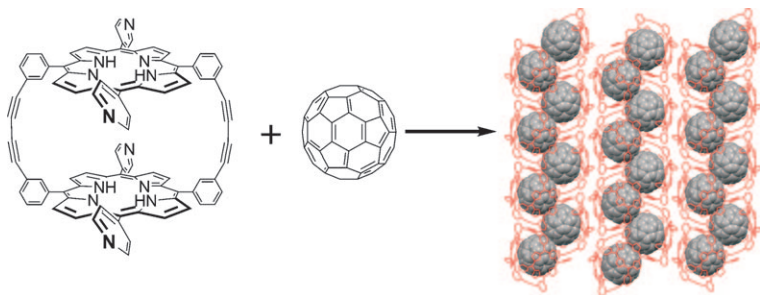
C–H Activation

A. Božović, S. Feil, G. K. Koyanagi,
A. A. Viggiano, X. Zhang,
M. Schlangen, H. Schwarz,*
D. K. Bohme* 11605–11610

Conversion of Methane to Methanol: Nickel, Palladium, and Platinum (d⁹) Cations as Catalysts for the Oxidation of Methane by Ozone at Room Temperature



Nickel is the best: The catalytic activity of M⁺ (M = Ni, Pd and Pt) in the oxidation of methane to methanol by ozone has been studied both experimentally and computationally. Ni⁺ is found to be the most efficient catalyst. The complete catalytic cycle with Ni⁺ has no poisoning side reactions and so proceeds, in principle, with an infinite turnover number.



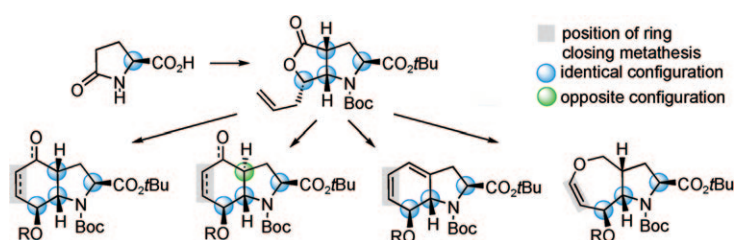
A zigzag array of C₆₀ is formed in the crystal structure of its inclusion complex with a cyclic free-base porphyrin dimer (see figure). The complex shows

photoinduced electron transfer, anisotropic charge mobility, and photovoltaic activity.

Inclusion Complexes

*H. Nobukuni, Y. Shimazaki, H. Uno, Y. Naruta, K. Ohkubo, T. Kojima, S. Fukuzumi, S. Seki, H. Sakai, T. Hasobe, F. Tani** 11611–11623

Supramolecular Structures and Photoelectronic Properties of the Inclusion Complex of a Cyclic Free-Base Porphyrin Dimer and C₆₀



Mycotoxins by metathesis: Ring-closing metathesis has been successfully employed for the construction of *cis*- and *trans*-annulated azabicyclic cyclohexenones, as well as an azabicyclic seven-membered cyclic enol ether (see

scheme; Boc = *tert*-butoxycarbonyl). These molecules are building blocks for a number of thiodiketopiperazine natural products. A unified synthetic strategy targeting these natural products is reported.

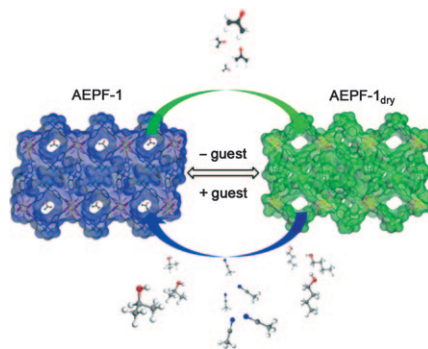
Natural Products

*U. Gross, M. Nieger, S. Bräse** 11624–11631

A Unified Strategy Targeting the Thiodiketopiperazine Mycotoxins Exserohilone, Gliotoxin, the Epicoccins, the Epicorazines, Rostratin A and Aranotin



Flexible friend: A dynamic structural transformation occurs when guest removal takes place from AEPF-1 by a crystal to crystal transformation to produce a new “dry” phase, AEPF-1_{dry} (see figure). Guest release occurs quickly and reversibly at room temperature. The special structural properties of this Ca-based metal–organic framework allow it to selectively adsorb organic solvents.



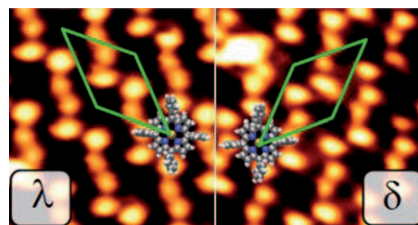
Metal–Organic Frameworks

*A. E. Platero-Prats, V. A. de la Peña-O’Shea, N. Snejko, Á. Monge, E. Gutiérrez-Puebla** 11632–11640

Dynamic Calcium Metal–Organic Framework Acts as a Selective Organic Solvent Sponge



Deformed porphyrins: The adsorption of Co-TPP on Cu(110) leads to the creation of highly deformed porphyrins that organise into chiral assemblies. Scanning tunnelling microscopy (see figure) and periodic density functional theory studies reveal that strong metal–molecule interactions unlock this unexpected porphyrin geometry. Chiral self-assembly is then driven by the π – π interactions made possible by the distortion.



Chiral Assembly

P. Donovan, A. Robin, M. S. Dyer, M. Persson, R. Raval** . . 11641–11652

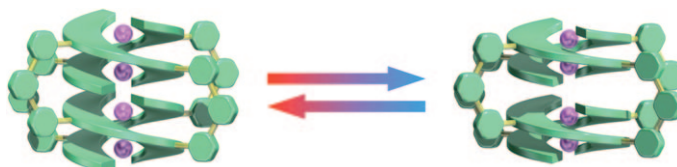
Unexpected Deformations Induced by Surface Interaction and Chiral Self-Assembly of Co^{II}-Tetraphenylporphyrin (Co-TPP) Adsorbed on Cu(110): A Combined STM and Periodic DFT Study



Supramolecular Chemistry

T. Hashimoto, T. Nishimura, J. M. Lim, D. Kim, H. Maeda* 11653–11661

Formation of Metal-Assisted Stable Double Helices in Dimers of Cyclic Bis-Tetrapyrroles that Exhibit Spring-Like Motion



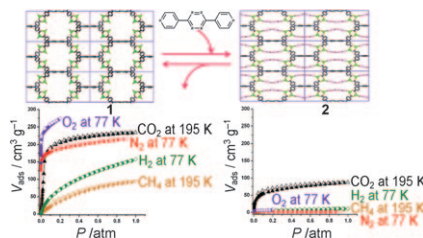
Molecular springs: Bidipyrin-bridged macrocycles, prepared from Ni^{II}-bridged coordination nanorings, yielded [2 + 4]-type Zn^{II}-driven twisted-ring dimers that exhibit tunable properties as a result of a spring-

like motion. The double helices behave as glue to connect two macrocycles and as the screws of hinges (see figure) to give thermally responsive synchronized spring systems.

Metal–Organic Frameworks

H. J. Park, Y. E. Cheon, M. P. Suh* 11662–11669

Post-Synthetic Reversible Incorporation of Organic Linkers into Porous Metal–Organic Frameworks through Single-Crystal-to-Single-Crystal Transformations and Modification of Gas-Sorption Properties

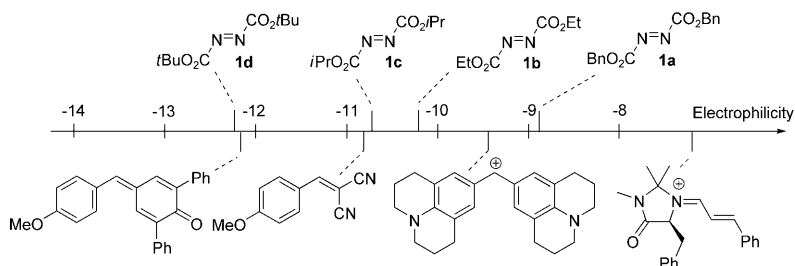


Constrained in one pot: The post-synthetic insertion of a 3,6-di(4-pyridyl)-1,2,4,5-tetrazine (bpta) bridging ligand into the metal–organic framework (MOF) **1** affords single-crystalline MOF **2**. Unlike its pristine form, the bpta ligand is significantly bent due to steric constraints. MOF **2** is prepared through a one-pot synthesis from which the bpta ligand is liberated to form single-crystalline **1**. Desolvated **1** adsorbs N₂, O₂, H₂, CO₂, and CH₄, whereas desolvated **2** exhibits selective adsorption of CO₂ (see picture).

Kinetics

T. Kanzian, H. Mayr* 11670–11677

Electrophilic Reactivities of Azodicarboxylates



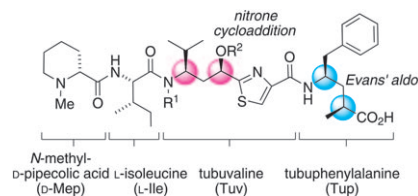
Electrophilic amination: Nitrogen electrophiles also follow the general correlation $\log k = s(N+E)$, originally developed for the reactions of carbon electrophiles with nucleophiles. The reaction rates of **1** with enamines were used to determine the empirical electrophilicity parameters, *E*, for **1a–d**

(see figure). Since the *E* parameters of **1** also correctly reproduce the rates of the reactions of **1** with Ar₃P, they can be used to predict the rate constants not only of the key step of organocatalytic α -aminations of carbonyl compounds, but also of the first step of the Mitsunobu reaction.

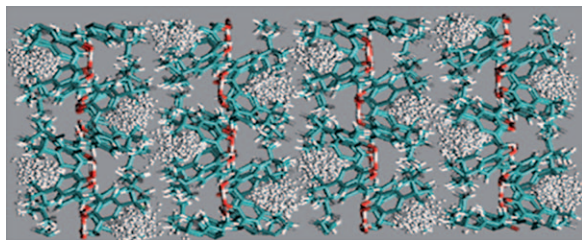
Stereoselectivity

T. Shibue, T. Hirai, I. Okamoto, N. Morita, H. Masu, I. Azumaya, O. Tamura* 11678–11688

Total Syntheses of Tubulysins



Antitumor activity: The total synthesis of tubulysins possessing potent anti-tumor activity has been accomplished. Key steps in the synthesis involved an 1,3-dipolar cycloaddition with double asymmetric induction (synthesis of Tuv, see scheme) and a stereoselective Evans aldol reaction (synthesis of Tup). These selective and scalable methods enabled the synthesis of sufficient quantities of tubulysins for biological assay.



What is in store? Experimental ^1H NMR peak intensity, direct adsorption measurements at different pressures, and grand canonical Monte Carlo simulations are used to determine adsorption isotherms of H_2 in

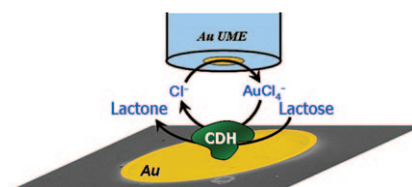
low-density *p*-*tert*-butylcalix[4]arene for pressures up to 175 bar (see figure). Small uptakes (not exceeding 0.25 mass % or one H_2 per calixarene bowl) inside the calixarene phase are detected.

Hydrogen Storage

*S. Alavi, * T. K. Woo, A. Sirjoosingh, S. Lang, I. Moudrakovski, J. A. Ripmeester** 11689–11696

Hydrogen Adsorption and Diffusion in *p*-*tert*-Butylcalix[4]arene: An Experimental and Molecular Simulation Study

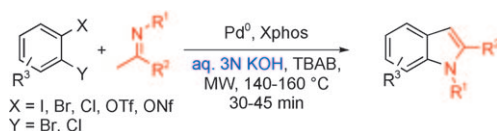
Biocatalytic deposition of gold nanoparticles was achieved by scanning electrochemical microscopy. A gold ultra-micro-electrode (UME) acts as a source of gold ions that are reduced by direct electron transfer from the enzyme cellobiose dehydrogenase (CDH) in the presence of β -D-lactose and deposited on a catalytic substrate such as palladium (see scheme).



Biocatalysis

*E. Malel, R. Ludwig, L. Gorton, D. Mandler** 11697–11706

Localized Deposition of Au Nanoparticles by Direct Electron Transfer through Cellobiose Dehydrogenase



A cascade “on water”: The Pd-catalyzed C–C/C–N cascade reaction between imines and *o*-disubstituted arenes to give polysubstituted indoles proceeds efficiently as a suspension in

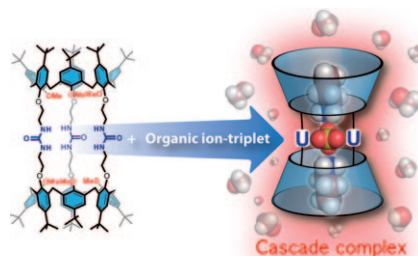
water under microwave irradiation (see scheme). These reaction conditions are clearly advantageous in comparison with the conventionally heated homogeneous process.

Domino Reactions

*J. Barluenga, * A. Jiménez-Aquino, F. Aznar, C. Valdés** 11707–11711

“On-Water,” Microwave-Assisted, Pd-Catalyzed Synthesis of Indoles from Imines and *o*-Difunctionalized Arenes

Calix[6]tubes: A tubular D_{3h} -symmetric calix[6]arene featuring two divergent hydrophobic cavities triply connected by short ureido linkages has been efficiently synthesized (see figure). This calix[6]tube displays unique host–guest properties towards neutral and charged species. In particular, this receptor can strongly bind organic ion triplets even in a markedly protic solvent and through a cooperative process.




Host–Guest Chemistry

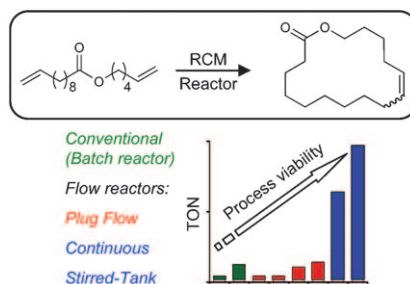
*S. Moerkerke, M. Ménand, I. Jabin** 11712–11719

Calix[6]arene-Based Cascade Complexes of Organic Ion Triplets Stable in a Protic Solvent

Ring-Closing Metathesis

S. Monfette, M. Eyholzer,
D. M. Roberge,*
D. E. Fogg* 11720–11725


 **Getting Ring-Closing Metathesis off the Bench: Reaction-Reactor Matching Transforms Metathesis Efficiency in the Assembly of Large Rings**

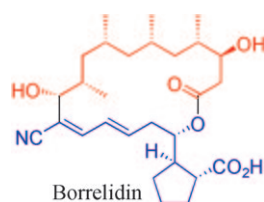


Go with the flow: Remarkably efficient ring-closing metathesis (RCM) macrocyclization is achieved by judicious matching of reaction and reactor. In a comparative study of batch, plug-flow, and continuous stirred-tank reactors, the last example enabled significantly higher yields and selectivity, in shorter reaction times, by using 25 × less catalyst (0.2 mol %) than the conventional batch reaction.

Natural Product Synthesis

A. V. R. Madduri,
A. J. Minnaard* 11726–11731

 **Formal Synthesis of the Anti-Angiogenic Polyketide (–)-Borrelidin under Asymmetric Catalytic Control**

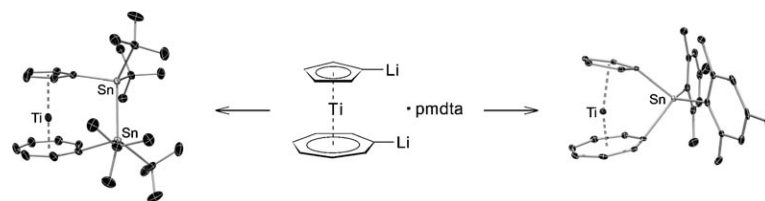


It's all under control: Catalysis control is used in a highly efficient formal total synthesis of the anti-angiogenic polyketide borrelidin (see structure). Asymmetric hydrogenation and asymmetric conjugate addition reactions are used as key steps in a synthesis that, due to high selectivity, does not require separation of stereoisomers.

Troticenophanes

H. Braunschweig,* M. Fuß,
S. K. Mohapatra, K. Kraft, T. Kupfer,
M. Lang, K. Radacki, C. G. Daniliuc,
P. G. Jones, M. Tamm* . . 11732–11743

Synthesis and Reactivity of Boron-, Silicon-, and Tin-Bridged *ansa*-Cyclopentadienyl–Cycloheptatrienyl Titanium Complexes (Troticenophanes)




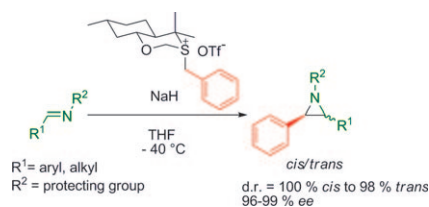
Bridge work: Reaction of $[\text{Ti}(\eta^5\text{-C}_5\text{H}_4\text{Li})(\eta^7\text{-C}_7\text{H}_6\text{Li})]\cdot\text{pmdta}$ (pmdta = pentamethyldiethylenetriamine) with $\text{Cl}_2\text{SnMes}_2$ (Mes = 2,4,6-trimethylphenyl) and $\text{Cl}_2\text{Sn}_2t\text{Bu}_4$ yields the stan-na[n]troticenophanes ($n = 1, 2$; see picture), which represent the first hetero-

leptic *ansa* complexes featuring Sn bridges. The title compounds exhibit a distinct reactivity with respect to oxidative addition reactions and are therefore promising precursors for further transformations.

Stereoselective Synthesis

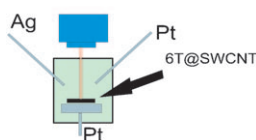
I. Dokli, I. Matanović,
Z. Hameršak* 11744–11752

 **Sulfur Ylide Promoted Synthesis of N-Protected Aziridines: A Combined Experimental and Computational Approach**



Selectivity explained: A range of N-protected aziridines were prepared in moderate to good yield and with high enantiomeric excess (*ee*) of both isomers from N-protected imines by using an oxathiane benzyl sulfonium salt (see scheme; Tf = triflate). An unusual *cis* selectivity was observed in the formation of *tert*-butyl-substituted aziridines and was explained by using computational investigations.

Sexithiophene doping: Sexithiophene encapsulated in single-walled carbon nanotubes (6T@SWCNT peapods, see figure, right) is prepared by a thermal reaction. The resulting material is studied by Raman spectroscopy and in situ Raman spectroelectrochemistry (see figure, left). The changes caused by the doping of SWCNTs and electrochemical charging are investigated.



Spectroelectrochemistry

M. Kalbáč, L. Kavan, S. Gorantla, T. Gemming, L. Dunsch* 11753–11759

Sexithiophene Encapsulated in a Single-Walled Carbon Nanotube: An In Situ Raman Spectroelectrochemical Study of a Peapod Structure



* Author to whom correspondence should be addressed



Supporting information on the WWW (see article for access details).



Full Papers labeled with this symbol have been judged by two referees as being “very important papers”.



A video clip is available as Supporting Information on the WWW (see article for access details).

SERVICE

Spotlights _____ 11512 Author Index _____ 11760 Keyword Index _____ 11761 Preview _____ 11763

Issue 37/2010 was published online on September 24, 2010

